Mon. Not. R. Astron. Soc. **000**, 000–000 (0000) Printed 5 February 2008 (MN LATEX style file v2.2)

Testing Dark Energy with the Advanced Liquid-Mirror Probe of Asteroids, Cosmology and Astrophysics

Pier Stefano Corasaniti,[1,2] Marilena LoVerde,[1,3] Arlin Crotts[1,2] and Chris Blake[4]
[1] *ISCAP, Columbia University, New York, NY 10027, USA*
[2] *Department of Astronomy, Columbia University, New York, NY 10027, USA*
[3] *Department of Physics, Columbia University, New York, NY 10027, USA*
[4] *Department of Physics & Astronomy, University of British Columbia, Vancouver, V6T 1Z1, Canada*

5 February 2008

ABSTRACT
The Advanced Liquid-Mirror Probe of Asteroids, Cosmology and Astrophysics (ALPACA) is a proposed 8-meter liquid mirror telescope surveying ~ 1000 deg^2 of the southern-hemisphere sky. It will be a remarkably simple and inexpensive telescope, that nonetheless will deliver a powerful sample of optical data for studying dark energy. The bulk of the cosmological data consists of nightly, high signal-to-noise, multiband light curves of SN Ia. At the end of the three-years run ALPACA is expected to collect $\gtrsim 100,000$ SNe Ia up to $z \sim 1$. This will allow us to reduce present systematic uncertainties affecting the standard-candle relation. The survey will also provide several other datasets such as the detection of baryon acoustic oscillations in the matter power spectrum and shear weak lensing measurements. In this preliminary analysis we forecast constraints on dark energy parameters from SN Ia and baryon acoustic oscillations. The combination of these two datasets will provide competitive constraints on the dark energy parameters under minimal prior assumptions. Further studies are needed to address the accuracy of weak lensing measurements.

Key words: cosmology: dark energy

1 INTRODUCTION

Over the past decade a picture of the Universe has emerged from a number of cosmological observations which have shed light on its geometry, matter content and clustering properties (De Bernardis et al. 2000; Percival et al. 2001; Spergel et al. 2003; Tegmark et al. 2004). Most astonishing amongst these findings is certainly the existence of "dark energy" which dominates the total energy density of the Universe and which is responsible for its present state of accelerated expansion (Riess et al. 1998; Perlmutter et al. 1999).

Despite the accurate measurements of the Cosmic Microwave Background anisotropies, the SN Ia luminosity distance observations and the detailed mapping of the large scale matter distribution, the nature of this exotic component still remains unknown and little progress has been made so far in this field, both at theoretical and observational level.

The cosmological constant has been advocated as the simplest candidate, since it is physically motivated representing the energy contribution of the vacuum. However we have no convincing explanation as to why the observed value is extremely small compared to particle physics expectations. Alternative scenarios have flourished in the recent past, although none seems to provide a consistent particle physics formulation. For a recent review see Padmanabhan (2005).

Supernova type Ia observations give the strongest evidence in favor of dark energy (Riess et al. 2004), nonetheless the limited number of measurements are still affected by large experimental and systematic uncertainties which prevent further insights. Consequently many questions about the properties of dark energy still remain unanswered. For instance it would be crucial to know whether the dark energy is time dependent or not, whether it clusters, whether its effects are caused by an exotic form of matter or by a different behavior of gravity on the large scales. Recent data analysis have shown that current observations lack the necessary accuracy to address these very issues (see for instance Corasaniti et al. 2004 and reference therein).

Complementary to the SN Ia observations, several other tests of dark energy have been studied in a vast literature including baryon acoustic oscillations in the galaxy power spectrum (Blake & Glazebrook 2003; Seo & Eisenstein 2003), cluster number counts (Weller & Battye 2003; Wang et al. 2004), weak lensing shear measurements (Hu & Jain 2004; Benabed & Van Waerbeke 2004) just to mention a few.

Improving the accuracy and reducing the systematics is the necessary condition for these methods to be effective. However they are all limited to some extent by degeneracies between dark energy and the other cosmological parameters. It is therefore unlikely that one single experiment may reveal the nature of dark energy. Progress seems only possible through a synergy of these different tests.

The Advanced Liquid-mirror Probe of Asteroids, Cosmology and Astrophysics (ALPACA) is a proposal for the realization of a ground based liquid-mirror telescope surveying a strip of sky of the southern-hemisphere. The survey will collect a huge amount of data divided in several datasets pertaining to SN Ia light curves, high redshift galaxies and weak lensing.

In this paper we study the constraints on dark energy from the estimated distribution of SN Ia observed during the nominal duration of the survey, and from the expected level of detection of the baryon acoustic oscillations in the galaxy power spectrum. The paper is organized as follows. In Section 2 we give an overview of the project. In Section 3 we discuss datasets that the survey is expected to provide, in particular SN Ia observations, baryon acoustic oscillations and weak lensing. In Section 4 we introduce the Fisher matrix analysis and in Section 5 we present our results. Finally in Section 6 we discuss our conclusions.

2 ALPACA PROJECT

ALPACA is an 8-meter liquid mirror telescope which will incorporate a 3°-wide imaging field and will be sited on Cerro Tololo (CTIO) in northern Chile. It is amazingly cost effective, delivering more information than virtually any competing survey instrument but at a small fraction of the cost. It will be a remarkably simple and inexpensive telescope that nonetheless will deliver powerful samples of optical data that are suitable for dark energy studies.

The concept of large, liquid-mirror telescope (LMT) is fairly new, although LMTs have successfully operated for over a decade (Cabanac, Borra & Beauchemin 1998; Hickson & Mulrooney 1998). Serious difficulties which compromised the past optical performance of LMT have now been eliminated. The result of these advancements in the liquid-mirror technology is seeing-dominated imaging. The next generation of LMT such as ALPACA can therefore compete with standard large optical telescopes for many projects.

ALPACA imaging quality is expected to be limited only by the seeing at CTIO, hence $\lesssim 1''$. The cosmological survey field will cover 775 deg^2 in five bands (u, b, r, i, z) with limiting nightly AB magnitudes in the range 23rd to 25th over a large fraction of the field. Four of the five photometric bands u (310-410nm), b (415-555nm), r (560-745nm) and i (750-1050nm) are spaced evenly in $log(\lambda)$ (λ being the wavelength), so that K-correction uncertainty vanishes at the special ratios of $(1 + z) = 1.25, 1.58$ and 1.98. A fifth band z (950-1050nm) is especially useful for isolating high-redshift objects. An additional $100 - 200$ deg^2 will be covered at lower sensitivity. ALPACA will observe the field passing directly overhead at CTIO, some 3° across, of which 2.5° are well suited for cosmological work. The focal plane's CCDs operate in drift-scan mode, each CCD reobserves the same strip of sky each night, making image subtraction and further analysis procedures stable, simple and redundant. We are also exploring installation of a multiobject spectrograph. The nominal duration of the survey is 3 years, at which time the flux depth will approach the crowding limit. The total amount of data collected during the three years run is expected to be of several petabytes.

Observations of SN Ia standard candle luminosity distance are expected to provide the bulk of the cosmological data, other datasets will include weak lensing, baryon oscillations, cluster number counts, strong-lens time delays, and cross-correlation multiple-waveband methods, such as ISW-correlation with CMB maps and X-ray galaxy clusters.

3 DATA PRODUCTS

3.1 SN Ia standard candles

Supernovae Type Ia light curves are related by one parameter family relation between the time-width and the maximum-light peak (Phillips 1993; Hamuy et al. 1996). As consequence of this SN Ia are standardizable candles and can be used as distance indicators (Riess, Press & Kirshner 1996; Perlmutter et al. 1997; Phillips 1999). Models of supernova have been intensely investigated for decades, but only in the past few years have three-dimensional numerical simulations provided a better understanding of the physical processes which take place during the explosive phase (see Hoflich et al. (2003) for a recent review).

The most accredited scenario consists of a carbon/oxygen (C/O) White Dwarf (WD) accreting material from an evolved companion star. As the WD reaches the Chandrasekar mass, the compressional heating triggers a thermo-nuclear explosion in the WD's core that propagates to the outer layers. However we still lack of a comprensive understanding of the fine details of the explosive phase which has limited the possibility to make robust quantitative predictions for the SNe light curves and spectra. In fact there is evidence that a number of secondary effects are responsible for deviations of the SN light curves from the one parameter family relation. These may depend on conditions prior to the explosion, such as the initial metallicity of the WD, the C/O ratio as function of the mass of the progenitors, and features of the explosive phase, such as rotational support, magnetic fields, convection structure in the deflagration front, viewing angle, ejecta asymmetries, effects of the companion on the ejecta, circumstellar interactions just to mention a few. Some of these may be purely stochastic, while others may leave clues in multiband lightcurves which will allow their induced variance to be removed or reduced. Several theoretical treatments have attempted to predict the effect on light curves of these various intrinsic factors (Hoflich, Wheeler & Thielemann 1998; Dominguez & Hoflich 2000; Mazzali et al. 2001; Pinto & Eastman 2001; Timmes et al. 2003). Unfortunately, they tend not to agree well on the size, sign or even the rough nature of these effects. In addition extrinsic effects, such as varying extinction laws or gravitational lensing may also influence the luminosity and other lightcurve observable as well.

The use of the brighter-slower relation has already allowed for a reduction of the dispersion in the magnitude-luminosity distance to $\sim 15\%$ r.m.s. (Phillips 1993, 1999;

Table 1. The redshift distribution of SN Ia expected from ALPACA, where z corresponds to the center of the bin.

z	0.1	0.19	0.28	0.37	0.46	0.55	0.64	0.73	0.82	0.91	1.0
N(z)	300	900	4500	9000	13500	19800	12600	12600	6750	4038	2204

Riess, Press & Kirshner 1996; Perlmutter et al. 1997; Goldhaber et al. 2001). Several studies have shown that this scatter can be further reduced using color data. For instance using the CMAGIC method (Wang et al. 2003) to find when $B-V$ color reaches a certain level after maximum light and thereby inferring luminosity, the dispersion can be limited to $8-10\%$. This method still requires an accurate measurement of the time-width of the maximum-light peak. On the contrary using the $B-V$ color 12 days after maximum-light (ΔC_{12}) can reduce the scatter to $\sim 7\%$ or less (Wang et al. 2005) without the need of the maximum-light peak width.

The ALPACA survey strategy is optimal for detecting a huge sample of supernovae, providing superlative quality dataset of nightly, high signal-to-noise, multiband SN Ia light curves. At the end of the three years run ALPACA is expected to observe $\gtrsim 100,000$ supernovae distributed in ten equally spaced redshift bins in the range $0.2 < z < 1$, and several hundred low-z supernova ($z < 0.2$). Hence a primary utility of the ALPACA dataset would be to improve the accuracy of the SN Ia standard candle relation and reduce systematic effects. In Table 1 we list the expected SN Ia redshift distribution.[1]

As discussed above, the theoretical uncertainties in the physics of SN Ia leave us without indication on how individual characteristics of the progenitors or peculiar conditions during the explosive phase may systematically affect the standard-candle relation. If such effects exist we can only hope to identify them through the component analysis of large sample of nightly, high S/N, multiband light curves. Although it is not *a priori* obvious which observational features might tie to luminosity, we might already have hints. For example, the CMAGIC technique (Wang et al. 2003) uses intensively sampled multiband lightcurves to produce a color-based correction to the maximum-light standard-candle relation. However there is still more information in such light curves. As an example, B-band "bump" of additional luminosity above the observed, or linear M_B versus $B-V$ evolution can add up to ~ 0.5 mag to the B luminosity near maximum light, which indeed seems to be at least roughly correlated with the SN peak luminosity. Such features might become manifest as additional higher order components to the brighter-slower relation. Using our high signal-to-noise, densely sampled, multicolor lightcurves, we expect to be able to measure from the component analysis even 4th and 5th-moments, and their possible correlations with luminosity.

Furthermore multiband lightcurve shape may be tied to the overall SN luminosity. For instance, it has been suggested that under multiple scattering conditions, light echoes can affect the effective luminosity and color of SNe Ia events (Patat 2005). Single scattering has negligible effect at the level of accuracy required in the SN Ia standard-candle relation, but in the case of optical-thickness of order of unity, circumstellar echoes may prove important even for SNe Ia near maximum light, to the point of affecting stretch or color-based luminosity corrections significantly. Such an echo will affect various bands differently, and may be or may not be associated with high extinction, depending on the patchiness of the surrounding dust. These characteristics makes ALPACA nightly multiband lightcurves an optimal benchmark to measure this effect.

In addition the large ALPACA dataset will allow us to search for possible subclasses of SN Ia and to the discovery of new standard-candle relations at different redshifts. Since we can already disentangle SN Ia from core-collapse SN via their multiband light curves alone (Johnson and Crotts 2005), we can simply rely on spectroscopy of a few representative members for characterization of each Ia subclass we discover (not necessarily for type classification of every SN). In fact hydrogen-rich supernova (Type II) can be distinguished from the hydrogen-poor (Ia, Ib and Ic) through the UV deficit, since UV radiation is blocked in Type I explosions by metal lines. Contamination from SN Ib/c can be particularly relevant at high redshift and affect the cosmological parameter estimation (Homeier 2005). Efficient photometric identification of Ib/c is also possible using four-band photometry focused on the bluer bands and with modest photometric accuracy (Gal-Yam et al. 2004). At the highest redshifts ($z \gtrsim 1$) weak lensing from the intervening mass distribution introduce a scatter of about 10% (with zero shift in mean), and even weak lensing maps can correct only a small fraction of this effect (Dalal et al. 2003). This scatter is much smaller at lower redshifts ($z < 1$) and can eventually be inferred from the data (Amanullah, Mortsell & Goobar 2003). Due to the large number of SN Ia per redshift bin this effect is negligible and averaged out.

A sample of tens or hundreds of SN Ia studied in this way might reveal the spectroscopic characteristics associated with these photometric properties. Furthermore, if we can also measure the redshifts of these SNe's host galaxies, we can derive accurate luminosities.

Although ALPACA is conceived as a drift-scanned imaging telescope, it is not impossible to suggest how a spectrograph might be introduced at a later time. This instrument would also drift scan, this time through the reimaging system of the spectrograph onto the time-delay integration (hence drift-scanned) CCD detector at the back of the spectrograph. A spectrographic slit mask could also be scanned across the focus of the telescope in front of the spectrograph in a way which might deliver many spectra simultaneously. The implementation of this idea might also deliver spectra for many thousands of supernovae, and could study huge numbers of galaxies as well.

Measuring the apparent brightness and host galaxy redshift for these supernovae would allow us to compute their luminosities to the level of 1% or better relative to other SN within redshift intervals of $\Delta z \approx 0.1$ (even given the current

[1] We thank Ben Johnsonn for computing the expected SN Ia redshift distribution.

uncertainty in the background cosmology). This will give us the opportunity to isolate samples of Type Ia SNe within redshift bins of $\Delta z \approx 0.1$. In one year's survey, each bin will contain thousand of SNe. Comparing these large samples of SNe of nearly identical redshifts (therefore nearly equidistant), will allow us to seek for subclasses of SNe Ia within each redshift bin. Such subclasses could be distinguished on the basis of temporal evolution in various bands (for example different expansion rates at the same peak luminosity would indicate different temperature evolutions beyond those implied by ^{56}Ni mass), or from higher-order moments of the light curves. If the fractional contributions of the various subclasses vary with redshift, we could then compensate for the effect. Furthermore, the various subclasses will be checked against one other to identify and correct for any systematic drifts within individual subclasses.

3.2 Baryon Acoustic Oscillations

Baryon oscillations in the galaxy power spectrum have recently emerged as a promising probe of dark energy (Blake & Glazebrook 2003; Seo & Eisenstein 2003). The large-scale linear clustering pattern contains a series of small-amplitude, roughly sinusoidal, modulations in power of identical physical origin to the acoustic peaks observed in the CMB. These oscillations encode a characteristic scale, the sound horizon at the drag epoch, which can be used as a cosmological standard ruler in the low-redshift Universe. When applied in the tangential and radial directions, this method enables the measurement of the angular diameter distance $D_A(z)$ and Hubble parameter $H(z)$ in units of the sound horizon, over a series of redshift slices, which in turn may be used to place accurate constraints on dark energy models.

The preferred scale was recently identified in the clustering pattern of Luminous Red Galaxies in the Sloan Digital Sky Survey (Eisenstein et al. 2005), constituting an important validation of the technique. A power spectrum analysis of the final 2-degree Field Galaxy Redshift Survey produced consistent results (Cole et al. 2005). The baryon oscillations method is robust against systematic errors. The underlying structure of acoustic peaks can be modeled very accurately using the linear physics of the CMB. In the galaxy distribution there are modifying "non-linear" effects owing to redshift-space distortions, halo bias and non-linear growth of structure. However, these effects are confined to broad-band changes to the power spectrum and do not introduce preferred scales that could be confused with the early-universe sound horizon. Recent simulations have confirmed that the baryon oscillation signature is preserved with only minor degradation (Seo & Eisenstein 2005, Angulo et al. 2005, Springel et al. 2005, White 2005). The acoustic signature may also be measured from photometric redshift surveys (Seo & Eisenstein 2003; Blake & Bridle 2004), although the smearing of radial information implies that only $D_A(z)$ can be determined with any confidence. However, given a sufficiently deep survey and accurate photometric redshifts, baryon oscillations may be detected with only ~ 1000 deg^2 of imaging in broad redshift slices centered at $z = 1$ and $z = 3$. We use the technique of (Blake & Bridle 2004) to simulate the resulting measurements of $D_A(z = 1)$ and $D_A(z = 3)$. The expected galaxy number guarantees that the clustering measurements are limited by cosmic variance and not by shot noise ($nP = 3$ in the notation of Seo & Eisenstein 2003). This is entirely consistent with the anticipated survey depth of ALPACA. We assume a survey area of 775 deg^2. For some galaxy classes, accurate photometric redshifts are possible with five broad bands, for Luminous Red Galaxies (Padmanabhan et al. 2005) $\sigma_z = \sigma_0(1 + z)$ with $\sigma_0 = 0.03$ at $z < 1$, due to the strong spectral break which implies rapidly changing colours with redshift. For other classes $\sigma_0 = 0.06$ (Fernandez-Soto et al. 2002), while good photometric performance should also be possible for $z = 3$ galaxies using the Lyman break. For a recent analysis see Ilber et al. (2006). We suppose that these accuracies are achievable over the ranges $0.5 < z < 1.5$ and $2.5 < z < 3.5$. (We omit $1.5 < z < 2.5$ given that photometric redshifts will not be accurate in this range in the absence of near-infra-red data). For comparison, we also display the equivalent measurements from a spectroscopic survey with the same configuration, using the method of Glazebrook & Blake (2005). Our results are listed in Table 2. An additional potential systematic error for an ALPACA large-scale structure survey is the survey geometry, which is a long, narrow stripe. Statistically, the number of measured Fourier modes is independent of the survey area. However, in order to robustly measure the clustering amplitude on a given scale, that scale must significantly exceed the minimum dimension of the survey. Otherwise we risk an enhanced cosmic variance owing to our consequent inability to measure the underlying large-wavelength modes in that dimension. In our case, the stripe width (2.5 deg, equivalent to a projected 101 Mpc/h at $z = 1$ and 194 Mpc/h at $z = 3$) is comparable to some of the scales of interest for baryon oscillations ($20 - 100$ Mpc). Further simulations are required to quantify the level of risk for enhanced cosmic variance.

3.3 Weak lensing and other datasets

ALPACA will also provide a very deep imaging survey perfectly suited for gravitational lensing studies. After three years of the survey, the cumulative AB magnitude limit in the r-band will be ~ 27, providing $\gtrsim 40$ gal/arcmin^2. The imaging quality will be limited only by seeing at the CTIO site, thus no worse than 1 arcsec. With this resolution ALPACA will be capable of mapping the dark matter distribution from cosmic shear measurements with unprecedent resolution. Small scale resolution (on the arcmin scales) combined with measurements up to 1° are particularly important to constrain dark energy. For a given amplitude of the scalar perturbations the balance between the non-linear scales and the large ones is sensitive to the dark energy parameters (Benabed & Van Waerbeke 2004). A more powerful method is to use lensing "tomography" (Hu 1999) from different redshift bins. ALPACA's sensitivity ensures that the noise coming from the intrinsic ellipticity of galaxies is negligible at all scales, offering an optimal measurement of gravitational lensing in the range of interest. A known source of limitation arises from the correction of galaxy shapes for Point Spread Function (PSF) effects. Foreground stars in the ALPACA stripes can be used to determine the anisotropic PSF and correct the images with standard techniques (Kaiser, Squire & Broadhurst 1995; Heymans et al. 2005). In contrast the isotropic PSF tends to circularize the

galaxy shape and therefore to dilute the lensing signal. In such a case a correction factor proportional to the seeing must be applied. A seeing $\lesssim 1''$ is necessary in order to keep the uncertainty of the shape correction factor below 5% (Erben et al. 2001). Improving the observational accuracy is not the only complication, on the theoretical side we have a limited knowledge of the growth of the non-linear structures. Using N-body simulations it has been possible to predict the non-linear power spectrum up to 1 arcmin with 5% accuracy at most (Smith et al. 2003).

An interesting characteristic of ALPACA is that the same region of the sky will be sampled ~ 1000 times. This is an entirely new regime of the PSF correction, which has never been explored before. In fact the number of dithered images with current lensing survey is ~ 10. The larger number of exposures could greatly help to better determine the effect of systematics. We leave the analysis of ALPACA weak lensing observations to future studies.

The survey will measure the location and collect photometric redshifts of $\sim 10^8$ galaxies over a large range of redshifts, potentially leading to the identifications of many galaxy clusters and groups. This will allow for an accurate number counting test, which in combination with existing measurements of Cosmic Microwave Background power spectrum can provide complementary constraints on the dark energy parameters (Wang et al. 2004). Another use of ALPACA would be to measure the cross-correlation between the survey and the CMB maps for measuring the Integrated Sachs-Wolfe (ISW) effect (Crittenden & Turok 1996). Although due to the limited sky coverage of the survey these measurements may not be able to provide competitive constraints on dark energy parameters (Pogosian et al. 2005). The survey will also provide a large sample of quasars for Alcock-Paczynski test (Calvao, De Mello Neto & Waga 2002), as well as strong-lens time delays (for 10-20 QSOs) (Shapiro 1964).

4 FISHER MATRIX ANALYSIS

We use the Fisher matrix approach to forecast constraints on dark energy parameters from ALPACA observations of SN Ia and acoustic baryon oscillations. The Fisher matrix provides a simple and practical method for estimating parameter errors. It gives a local approximation to the likelihood surface about a fiducial model for a set of independent observations (Tegmark, Taylor & Heavens 1997). Formally the Fisher matrix reads as

$$F_{\mu\nu} = \sum_i \frac{1}{\sigma^2(\mathcal{O}_i)} \frac{d\mathcal{O}_i}{d\theta_\mu} \frac{d\mathcal{O}_i}{d\theta_\nu}, \quad (1)$$

where θ_μ are the model parameters, $\mathcal{O}_i$ are the observations of the quantity $\mathcal{O}$ and $\sigma(\mathcal{O}_i)$ the experimental errors. The derivatives in Eq. (1) are computed at the fiducial model parameter values. The covariance matrix is given by the inverse of Fisher matrix, $C = F^{-1}$, with the one sigma errors on the model parameters given by the diagonal components, $C_{\mu\mu} = \sigma^2_{\theta_\mu}$. In case of multiple independent datasets the combined constraints can be inferred by simply adding the Fisher matrices of each experiment.

Supernova Ia observations measure the luminosity distance d_L through the standard-candle relation,

$$m(z) = \mathcal{M} + 5 \log \mathcal{D}_L(z), \quad (2)$$

where $\mathcal{M} \equiv M - 5 \log H_0 + 25$ is the "Hubble-constant-free" absolute magnitude and $\mathcal{D}_L(z) \equiv H_0 d_L(z)$ is the "Hubble-constant-free" luminosity distance. In flat universe the luminosity distance is given by

$$d_L(z) = (1+z) \int_0^z \frac{dz'}{H(z')}, \quad (3)$$

with

$$H(z) = H_0 \left[(1-\Omega_m) f_{DE}(z) + \Omega_m (1+z)^3 \right]^{1/2}, \quad (4)$$

where Ω_m is the dark matter energy density and

$$f_{DE}(z) = exp \left\{ 3 \int_0^z \frac{1+w(z')}{1+z'} dz' \right\} \quad (5)$$

with $w(z)$ being the dark energy equation of state. Several parameterizations have been extensively studied in the literature, for simplicity we limit our analysis to dark energy models parametrized by (Chevallier & Polarski 2001; Linder 2003):

$$w(z) = w_0 + w_a \frac{z}{1+z}. \quad (6)$$

We have a three-parameter space consisting of Ω_m, w_0 and w_a. In addition the magnitude-luminosity distance relation depends on the off-set parameter $\mathcal{M}$ which we marginalize over. For the fiducial cosmology we adopt a model with $\Omega_m = 0.3$, $w_0 = -1$ and $w_a = 0$. We compute the SN Ia Fisher matrix using Eq. (1) and the derivatives of $d_L(z)$ with respect to the model parameters using double-finite differences about the fiducial model.

We account for the uncertainty of the observed magnitude in each redshift bin, using the standard approach of adding in quadrature the statistical and the irreducible systematic errors (see for instance Kim et al. (2004)),

$$\sigma^2(z_i) = \frac{\sigma^2_{stat}}{N_i} + \sigma^2_{sys}, \quad (7)$$

with $\sigma_{stat} = 0.15$ and N_i being the number of SN Ia in the i-th bin. Assessing the amplitude of the expected level of systematic uncertainty σ_{sys} is more difficult. Because observations at higher redshift are more challenging the systematic error should increase, this increase is usually assumed to vary linearly with the redshift,

$$\sigma_{sys} = \delta m \frac{z}{z_{max}}, \quad (8)$$

where δm is the amplitude of the systematics at the maximum redshift bin of the survey z_{max}. As we have discussed in Section 3.1, we still lack robust quantitative prediction for SN Ia light curves and spectra. Although results from numerical simulations remain controversial, they seem to suggest that nightly high signal-to-noise multiband SN Ia light curves may suffice to reduce systematic uncertainties to few % level (see for instance Hoflich, Wheeler & Thielemann 1998). The use of multiple methods on a vast SN Ia sample such as the one provided by ALPACA is likely to reduce the level of systematics to $5-7\%$ or better. Constraints from future SN Ia survey usually assume a more optimistic 2% uncertainty. We forecast constraints for both $\delta m = 0.05$ and 0.02.

As discussed in Section 3.2, baryon acoustic oscillations in the matter power spectrum provide a standard ruler which

Table 2. Expected uncertainties on $x = (1+z)d_A(z)/s$ and $x' = H^{-1}(z)/s$ in different redshift bins, for different redshift measurements.

z	σ_x ($\sigma_0 = 0.03$)	σ_x (spect-z)	$\sigma_{x'}$ (spect-z)
1.0	0.039	0.013	0.022
3.0	0.020	0.009	0.016

can be used to infer cosmological distance measurements. Oscillations in the tangential component of the matter power spectrum give the comoving angular diameter distance at the redshift slice of the survey in units of the sound horizon,

$$x(z) = (1+z)\frac{d_A(z)}{s}, \tag{9}$$

where $d_A(z) = d_L(z)/(1+z)^2$ is the angular diameter distance and the sound horizon s is given by

$$s = \int_0^{a_{drag}} \frac{c_s}{\sqrt{\Omega_m a + \Omega_r}} da, \tag{10}$$

where a_{drag} is the value of scale factor at the epoch of baryon-drag (baryons decoupling) and Ω_r is the radiation energy density. The sound speed of the barotropic fluid is

$$c_s^2 = \frac{1}{3}\frac{1}{1+\frac{3}{4}\frac{\Omega_b}{\Omega_r}a}. \tag{11}$$

Oscillations in the radial component give the Hubble rate in units of the sound horizon,

$$x'(z) = \frac{H^{-1}}{s}. \tag{12}$$

Because of the dependence on the sound horizon, the parameter space is extended to Ω_b and the Hubble constant $h = H_0/100$. Again we use Eq. (1) to compute the Fisher matrix components. The expected errors on x and x' from ALPACA measurements are listed in Table 2.

5 RESULTS

We now discuss the results of the Fisher matrix analysis. We list in Table 3 and Table 4 the 1σ limits on Ω_m, w_0 amd w_a from SN Ia with $\delta m = 0.05$ and 0.02 systematic uncertainty respectively. We also quote the errors inferred from assuming the standard prior $\sigma_{\Omega_m} = 0.03$ and compare with those obtained combining baryon acoustic oscillations.

Supernova data alone poorly constrain the dark energy parameters due to the degeneracy in Ω_m, for instance for $\delta m = 0.05$, we find $\sigma_{\Omega_m} = 0.62$, $\sigma_{w_0} = 0.49$ and w_a unbounded. These errors reduce by nearly a factor 2 for the case $\delta m = 0.02$ (Table 4). On the contrary assuming the standard Ω_m prior we obtain $\sigma_{w_0} = 0.2$ and $\sigma_{w_a} = 1.1$ for $\delta m = 0.05$, and $\sigma_{w_0} = 0.11$ and $\sigma_{w_a} = 0.53$ for $\delta m = 0.02$.

Constraints on dark energy from baryon acoustic oscillations are also limited by degeneracies with other cosmological parameters, in particular Ω_m and h. In addition there is a further uncertainty due to the dependence on Ω_b which determines the size of the sound horizon at decoupling. Assuming these parameters to be perfectly known we find $\sigma_{w_0} = 0.17$ and $\sigma_{w_a} = 0.70$ for spectroscopic redshift measurements. In figure 1 we plot the 1σ contours in the $w_0 - w_a$ plane from SN Ia (solid line) and baryon oscillations (dash-dot line).

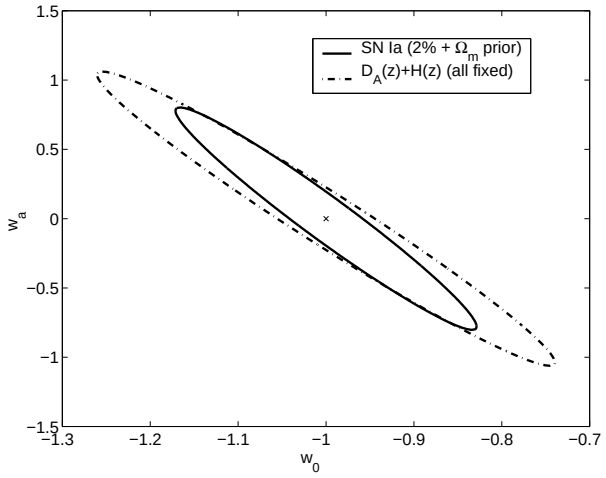

Figure 1. 1-σ Fisher matrix contours on $w_0 - w_a$. The solid line corresponds to SN Ia with 2% systematic uncertainty and 3% Gaussian prior on Ω_m, while the dash-dot line corresponds to BAO measurements with spectroscopic redshift accuracy assuming perfect knowledge of Ω_m and h.

We are particularly interested in the SN and BAO combined constraints, so as to determine how the combination of the baryon acoustic oscillations can realistically improve the dark energy limits from SN Ia under minimal prior assumptions. In such a case we only assume a Gaussian prior on the baryon density, $\sigma_{\Omega_b} = 0.006$ consistently with WMAP/BBN results (Spergel et al. 2003; Hansen et al. 2002) and h to be fixed.

In the case of photometric redshifts, the combination of SN Ia and BAO gives $\sigma_{\Omega_m} = 0.01$, $\sigma_{w_0} = 0.19$ and $\sigma_{w_a} = 0.96$ for $\delta m = 0.05$, and $\sigma_{\Omega_m} = 0.01$, $\sigma_{w_0} = 0.11$ and $\sigma_{w_a} = 0.52$ for $\delta m = 0.02$. The use of spectroscopic redshifts leads to slightly better constraints, for instance we find $\sigma_{\Omega_m} = 0.003$, $\sigma_{w_0} = 0.14$ and $\sigma_{w_a} = 0.58$ for $\delta m = 0.05$, and $\sigma_{\Omega_m} = 0.002$, $\sigma_{w_0} = 0.09$ and $\sigma_{w_a} = 0.43$ for $\delta m = 0.02$. The level of detection of baryon acoustic oscillations as expected for ALPACA will provide poor information on dark energy beyond that which comes from better constraining Ω_m to the level expected from future CMB experiments. In Table 5 we list the expected parameter errors from combining SN and BAO with CMB limits from Planck, the inferred constraints are compatible with those obtained in (Linder 2005). Including the shear weak lensing can certainly improve these limits, we leave this to a future study.

6 CONCLUSIONS

Uncovering the nature of dark energy is the new challenge of modern observational cosmology. Over the upcoming years lots of effort will be dedicated to improving luminosity distance measurements of SN Ia standard candles and extend observations to complementary dark energy tests, such as baryon acoustic oscillations and cosmic shear weak lensing. In order to accomplish such a program several experiments have been proposed both from ground and space.

Here we have presented the ALPACA survey and described the main datasets that the project is expected to

Table 3. 1-σ uncertainties on Ω_m, w_0 and w_a from SN Ia assuming 5% systematic error with Gaussian Ω_m prior and with different combinations of BAO detections.

	SN Ia ($\delta m = 0.05$)	$+\sigma_{\Omega_m} = 0.03$	$+D_A(z)$ ($\sigma_0 = 0.03$)	$+D_A(z) + H(z)$ (spect-z)
σ_{Ω_m}	0.62	-	0.01	0.003
σ_{w_0}	0.49	0.2	0.19	0.14
σ_{w_a}	-	1.1	0.96	0.58

Table 4. As in Table 3 with 2% SN Ia systematic error.

	SN Ia ($\delta m = 0.02$)	$+\sigma_{\Omega_m} = 0.03$	$+D_A(z)$ ($\sigma_0 = 0.03$)	$+D_A(z) + H(z)$ (spect-z)
σ_{Ω_m}	0.30	-	0.01	0.002
σ_{w_0}	0.20	0.11	0.11	0.09
σ_{w_a}	-	0.53	0.52	0.43

provide. The bulk of the data is represented by high signal-to-noise, multiband, nightly SN Ia light curves. At the end of the three year run ALPACA is expected to observe $\gtrsim 100,000$ supernovae distributed in the range $0.2 < z < 1$ and several hundreds at lower redshifts. This huge dataset will be useful for finding possible subclass of SN Ia at different redshifts and correlations in the multiband light curves beyond the brighter-slower relation. This will allow for calibration of the standard-candle relation and reduction of the systematic uncertainties.

In this paper we have forecasted limits on dark energy parameters from the expected redshift distribution of SN Ia and the detection of baryon acoustic oscillations in the matter power spectrum. Although the accuracy of BAO measurements cannot compete with dedicated surveys such as KAOS (Dey & Boyle 2003) or LSST (Tyson & Angel 2001), combining them with SN Ia data will provide competitive constraints under minimal prior assumptions. ALPACA will also deliver several other datasets and will be particularly suitable for weak lensing measurements.

ALPACA stakes out a regime in survey parameter space that is unique and useful, the intensive nightly, multiband monitoring of fields of order 1000 deg^2. While in principle other surveys such as LSST, Pan-STARRS, JDEM or DES are instrumented for such intensive monitoring, in practice they are driven by other motivations such as all-sky transient monitoring or weak-lensing mapping, devoting much less time than ALPACA to the 1000 deg^2 goal. Indeed, using these like ALPACA would be inefficient, since ALPACA is extremely economical for this application compared to one of these more flexible instruments. Liquid-mirror techniques have now reached such a high level of quality that liquid-mirror telescopes may be used for astrophysics and cosmology. The ALPACA project will take advantage of this and provide high quality data at a fraction of the cost of standard 8-meter telescopes or space missions. The vast possibilities of the ALPACA survey are still not fully explored and further investigation is needed.

ACKNOWLEDGMENTS

We are grateful to all members of the ALPACA collaboration and we are particularly thankful to David Branch, Paul Hickson, Ben Johnson, Ken Lanzetta, Nick Suntzeff, Jun Zhang, Yun Wang and Ludovic van Waerbeke for useful discussions and suggestions. P.S.C. is supported by Columbia Academic Quality Fund.

REFERENCES

Amanullah, R, Mortsell, E, Goobar, A., 2003, Astron. & Astrophys., 397, 819
Angulo, R. et al., 2005, Mon. Not. Roy. Astron. Soc. Lett., 362, L25
Benabed, K., Van Waerbeke, L., 2004, Phys. Rev. D, 70, 123515
Blake, C., Glazebrook, K., 2003, Astrophys. J., 594, 665
Blake, C., Bridle, S., 2004, astro-ph/0411713
Cabanac, R. A., Borra, E. F., Beauchemin, M., 1998, Astrophys. J., 509, 309
Calvao, M. O., De Mello Neto, J. R. T., Waga, I., 2002, Phys. Rev. Lett., 88, 091302
Chevallier, M., Polarski, D., 2001, Int. J. Mod. Phys. D, 10, 213
Cole, S. et al., 2005, Mon. Not. Roy. Astron. Soc., 362, 505.
Corasaniti, P. S., Kunz, M., Parkinson, D., Copeland, E. J., Bassett, B. A., 2004, Phys. Rev. D, 70, 083006
Crittenden, R. G., Turok, N., 1996, Phys. Rev. Lett., 76, 575
Crotts, A. et al., astro-ph/0507043
Dalal, N., Holz, D. E., Chen, X., Frieman, J. A., 2003, Astrophys. J., 585, L11
De Bernardis, P. et al., 2000, Nature, 404, 955
Dey, A., Boyle, B. editors, 2003, KAOS Purple Book
Dominguez, I., Hoflich, P., 2000, Astrophys. J., 528, 854
Eisenstein, D. et al., astro-ph/0501171
Erben, T. et al., 2001, Astron. & Astrophys.. 366, 717
Fernandez-Soto et al., 2002, Mon. Not. R. Astron. Soc., 330, 889
Gal-Yam, A. et al., 2004, Publ. Astron. Soc.Pac. in press, astro-ph/0403296
Glazebrook, K., Blake, C., 2005, astro-ph/0505608
Goldhaber, G., et al., 2001, Astrophys. J., 558, 359
Hamuy, M. et al., 1996, Astrophys. J., 112, 2391
Hansen, S.H. et al., 2002, Phys. Rev. D, 65, 023511
Heymans, C. et al., astro-ph/0506112.
Hickson, P., Mulrooney, M. K., 1998, Astrophys. J. Supp., 115, 35
Hoflich, P., Wheeler, J. C., Thielemann, F. K., 1998, Astrophys. J., 495, 617

Table 5. As in Table 4 with Planck.

	SN Ia + BAO (spect-z) + Planck
σ_{Ω_m}	0.001
σ_{w_0}	0.07
σ_{w_a}	0.31

Hoflich, P. A., Gerardy, C., Linder, E., Marion, H., astro-ph/0301334
Homeier, N. L., 2005, Astrophys. J., 620, 12
Hu, W., 1999, Astrophys. J., 522, L21.
Hu, W., Jain, B., 2004, Phys. Rev. D, 70, 043009
Ilbert, O., et al., 2006, astro-ph/0603217
Johnson, B., Crotts, A., 2005, astro-ph/0511377
Kaiser, N., Squires, G., Broadhurst, T., 1995, Astrophys. J., 449, 460.
Kim, A. G., Linder, E. V., Miquel, R., Mostek, N., 2004, Mont. Not. Roy. Astron. Soc., 347, 9091
Linder, E. V., 2003, Phys. Rev. Lett., 90 91301
Linder, E. B., 2005, astr-ph/0507263
Mazzali, P. et al., 2001, Astrophys. J., 547, 988
Padmanabhan, N. et al., 2005, Mon. Not. Roy. Astron. Soc., 359, 237
Padmanabhan, T., 2005, Curr. Sci., 88, 1057
Patat, F., 2005, Mont. Not. Roy. Astron. Soc., 357, 1161
Percival, W. J. et al., 2001, Mont. Not. Roy. Astron. Soc., 327, 1297
Perlmutter, S., et al., 1997, Astrophys. J., 483, 565
Perlmutter, S. et al., 1999, Astrophys. J., 517, 565
Phillips, M. M., 1993, Astrophys. J., 413, L105
Phillips, M. M., 1999, Astrophys. J., 118, 1766
Pinto, P. A., Eastman, R. G., 2001, New Astron., 6, 307
Pogosian, L. et al., 2005, Phys. Rev. D, 72, 103519
Prichet, C.J., astro-ph/0406242
Riess, A. G., Press, W. H., Kirshner, R. P., 1996, Astrophys. J., 473, 88
Riess, A. G. et al.. 1998, Astrophys. J., 116, 1009
Riess, A. G. et al., 2004, Astrophys. J., 607, 665
Seo, H.-J., Eisenstein, D. J., 2003, Astrophys. J., 598, 720
Shapiro, I. I., 1964, Phys. Rev. Lett., 13, 789
Smith, R. E. et al., 2003, Mont. Not. R. Astron. Soc., 341, 1311
Sollerman, J. et al., astro-ph/0510026
Spergel, D. N. et al., 2003, Astrophys. J. Suppl., 148, 175
Springel, V. et al, 2005, Nature, 435, 629
Tegmark, M., Taylor, M. N., Heavens, A. F., 1997, Astrophys. J., 480, 22
Tegmark, M. et al., 2004, Astrophys. J., 606, 70
Timmes, F. X., Brown, E., Truran, J. W., 2003, Astrophys. J., 590, L83
Tyson, J. A., Angel, R., 2001, ASP Conference Series, R. Clowes (ed), 232, 347
Wang, L. F., Goldhaber, G., Aldering, G., Perlmutter, S., 2003, Astrophys. J., 590, L43
Wang, S., Khoury, J., Haiman, Z., May, M., 2004, Phys. Rev., 70, 123008
Wang, X., Wang, L. F., Zhou, X., Lou, Y.-Q., Li, Z., 2005, Astrophys. J., 620, L87
Weller, J., Battye, R. A., 2003, New Astronomy Reviews, 47, 775
White, M., astro-ph/0507307